Air–Sea Interactions of Relevance to the ITCZ: Analysis of Coupled Instabilities and Experiments in a Hybrid Coupled GCM

TIANMING LI

University Corporation for Atmospheric Research, Visiting Scientist Program, Naval Research Laboratory, Monterey, California

(Manuscript received 30 October 1995, in final form 24 June 1996)

ABSTRACT

The eastern Pacific and Atlantic have a curious climatic asymmetry relative to the equator. Whereas the intertropical convergence zone (ITCZ) characterized by persistent and heavy rainfall and the warmest surface waters reside north of the equator, a cold tongue in sea surface temperature (SST) occurs at and south of the equator even though the time-mean solar radiation is approximately symmetric about the equator. In this paper the author investigates the relative role of three types of coupled ocean–atmosphere interaction processes—the meridional wind–SST feedback, the evaporation–wind feedback, and the low-level stratus cloud–SST feedback—in determining the climatic asymmetry relative to the equator.

This study has two components. First, a simple analytical model is constructed in which the aforementioned three positive-feedback mechanisms are all included in a unified dynamic framework. The author's stability analysis indicates that in a reasonable parameter regime the growth rates associated with the three coupled instabilities are of the same order of magnitude, suggesting that they are all important in contributing to the climatic asymmetry. Because of the dependence of the three feedback mechanisms on the existence of a shallow oceanic mixed layer that, in turn, is a result of equatorial easterlies, the existence of the equatorial easterlies is essential for the amplification of the climatic asymmetry.

Next, a hybrid coupled general circulation model is used in which a realistic continental and coastal geometry is presented. The model starts from an ideal symmetric condition forced only by the annual-mean insolation at the top of the atmosphere which is approximately symmetric about the equator. In the presence of the three air–sea interaction mechanisms, the coupled model is capable of reproducing a realistic asymmetric time-mean state in the eastern Pacific and Atlantic. The fundamental cause of the asymmetry in the eastern Pacific is the tilt of the western coast of the Americas, which perturbs SST in the vicinity of the coastal region through a so-called coastal wind-upwelling mechanism. The asymmetry in the Atlantic, on the other hand, results from the land–ocean thermal contrast between the bulge of northwestern Africa and the ocean to the south. The ocean–atmosphere interactions act as an amplifier to amplify the asymmetry set up by the continental or coastal asymmetry. Numerical experiments presented here demonstrate the importance of the geographic asymmetries and the ocean–atmosphere interactions in determining the preferred climatic position for the ITCZ.

1. Introduction

The eastern Pacific and Atlantic have a curious climate asymmetry relative to the equator. Whereas the atmospheric intertropical convergence zone (ITCZ) characterized by persistent and heavy rains and the warmest surface waters occur north of the equator (in the region of 8°N), a strong cold tongue in sea surface temperature (SST) appears at and south of the equator, even though annual-mean solar radiation is approximately symmetric about the equator.

Recent efforts to understand this curious phenomenon leads to new observational and theoretical discoveries. The heart of these discoveries lies in the interactions between the ocean and atmosphere that support a number of modes that are antisymmetric about the equator and can, through various feedback processes, convert a symmetric condition to an asymmetric one.

So far, three types of coupled ocean–atmosphere instabilities relevant to the phenomenon under discussion have been proposed. They all involve positive feedbacks between the ocean and atmosphere.

The first type of coupled ocean–atmosphere instability involves a positive feedback between the meridional wind and SST. This mechanism was originally hypothesized by Mitchell and Wallace (1992) based on observational evidence and further investigated by Chang and Philander (1994) in theory. This coupled ocean–atmosphere instability has a dominant antisymmetric mode that is different from symmetric modes [e.g., the delayed oscillator mode proposed by Schopf and Suarez (1988) and the slow SST mode suggested by Neelin (1991)] associated with the El Niño–Southern Oscillation. The

Corresponding author address: Dr. Tianming Li, Naval Research Laboratory, 7 Grace Hopper Avenue, Monterey, CA 93943.
E-mail: li@nrlmry.navy.mil

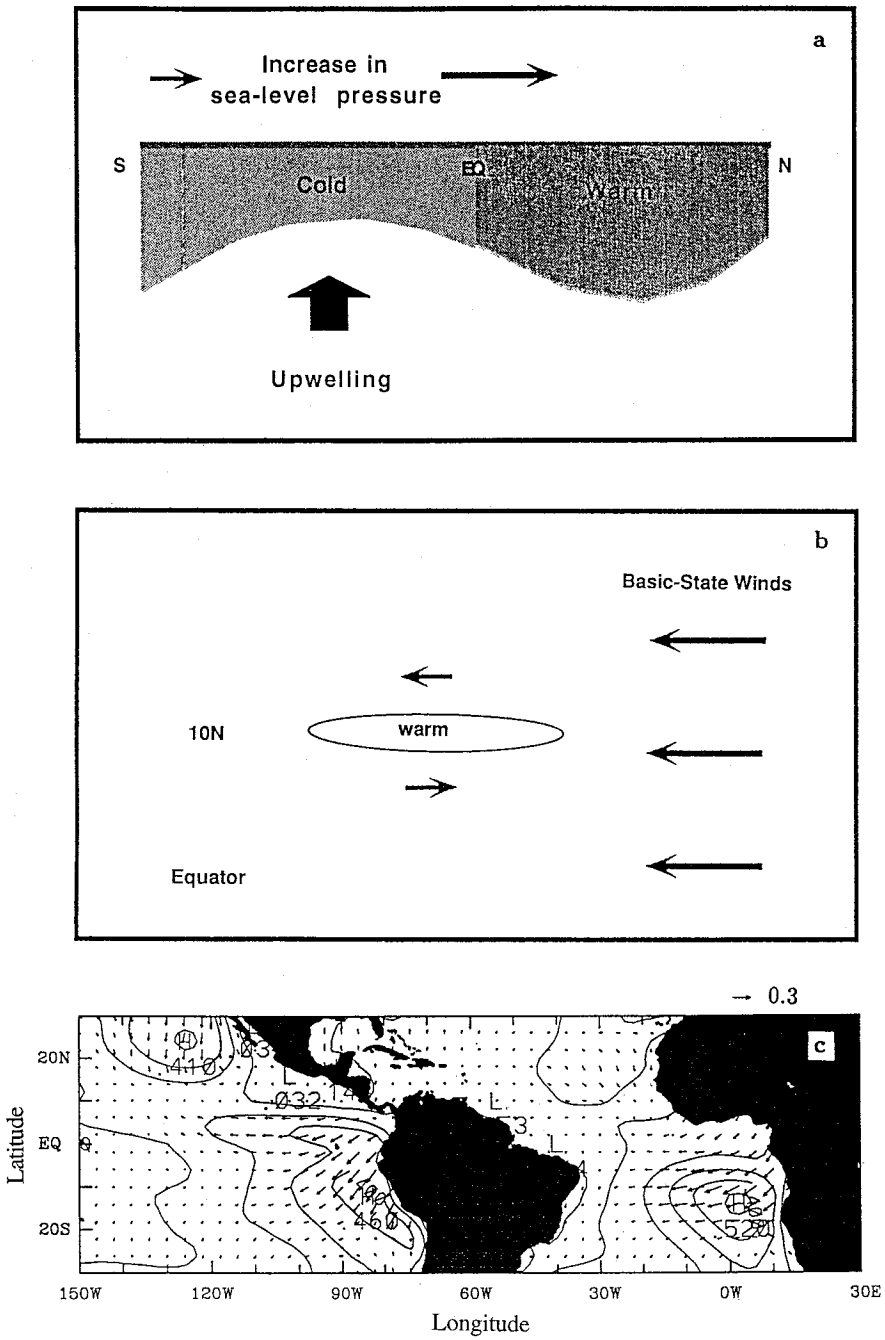

FIG. 1. Schematic diagrams showing (a) the coupled ocean–atmosphere instability of the first kind, the positive feedback between the meridional wind and SST, proposed by Mitchell and Wallace (1992) and Chang and Philander (1994), and (b) the coupled ocean–atmosphere instability of the second kind, the evaporation–wind feedback (Xie and Philander 1994). (c) ISCCP monthly mean stratus cloud fields. Contours represent the annual mean field and vectors represent annual harmonics (upward denotes a maximum amplitude in January, rightward in April, and so on).

mechanism of this coupled ocean–atmosphere instability can be demonstrated by using the schematic diagram shown in Fig. 1a. Suppose we start from a perfectly symmetric world in which maximum SST lies on the equator. Then, we introduce a small perturbation relative to the symmetric condition, a perturbation that displaces the warmest waters, initially at the equator, slightly northward. The southerly winds that converge onto the displaced warmest water, over which convection occurs, drive the oceanic currents with a northward component.

The northward oceanic currents are small far away from the equator because the Coriolis force deflects the wind-driven ocean currents. As the equator is approached, the northward currents gain in speed and reach a maximum value on the equator where the Coriolis force vanishes. It turns out that the oceanic surface currents are divergent south of the equator but convergent to the north. The divergent currents expose cold water from below to the surface and cool SST. The cooling in the ocean surface increases local sea level pressure and intensifies the northward pressure gradient, which further increases the northward winds. The intensified northward winds induce even stronger ocean upwelling south of the equator. Therefore, there is a positive feedback cycle between the atmosphere and ocean. Through this positive feedback cycle, the symmetric condition is destroyed and an asymmetric condition is established.

The second type of instability involves the positive feedback between evaporation and wind. This mechanism was originally proposed by Neelin et al. (1987) and Emmanuel (1987), in the zonal direction, to study the atmospheric low-frequency oscillation—the Madden–Julian oscillation. It was further investigated by Xie and Philander (1994) and Xie (1994), in a north–south direction, to study the climate asymmetries relative to the equator. The key to this mechanism lies in a basic-state wind distribution, depicted in Fig. 1b. Suppose initially we have an SST perturbation located at 10°N. In response to the SST forcing, westerly (easterly) wind anomalies are generated to the south (north) of the SST perturbation. The westerly anomalies to the south tend to reduce the surface evaporation because the basic-state winds are easterlies, which causes a positive time-change rate for SST. As a result, the SST anomaly intensifies and propagates equatorward. Near the equator, strong oceanic upwelling induced by basic-state easterlies causes the extremely cold SST, which suppresses the atmospheric convection and prevents further equatorward movement of the ITCZ. Therefore, the maximum SST and convection have to stay along a certain latitude away from the equator. Without the equatorial cold tongue, a case in the western Pacific, the maximum SST and ITCZ could finally reach and stay at the equator.

The third type of coupled instability involves the positive feedback between the low-level marine stratus clouds and SST (Li and Philander 1996; Philander et al. 1996). Whereas the convective clouds favor the warmest waters in the western Pacific, the low-level stratus clouds form over very cold water in the eastern Pacific (Fig. 1c). These stratus clouds vary seasonally and have maximum values during the early northern fall when the SST is lowest. The low-level stratus clouds are particularly important in a coupled ocean–atmosphere system because they are involved in a positive feedback cycle: the lower the SST, the larger the static stability of the lower troposphere, the stronger the atmospheric inversion, the thicker the deck of low-level stratus clouds; the increase in the clouds further shields the ocean from shortwave radiation and causes even lower SST. An analysis of observed climatological monthly mean data reveals that there is a negative correlation between the stratus clouds and SST in the eastern tropical Pacific and Atlantic. With a decrease in SST, the low-level stratus clouds increase dramatically, which further reduces the shortwave radiation into the ocean and results in a colder SST.

The discovery of these ocean–atmosphere interaction processes substantially advances our understanding of the observed phenomenon. However, the relative importance of these mechanisms is not clear so far. Previous studies isolated different processes. It is necessary to combine all the processes together in a unified dynamic framework.

This study is a twofold effort: 1) to build a simple analytical model and to analyze and compare the growth rates associated with the three coupled ocean–atmosphere instabilities and 2) to use a more sophisticated hybrid coupled GCM, in which a realistic geographic distribution is described, to understand the processes that initiate an equatorial asymmetry and the air–sea interaction mechanisms that amplify the asymmetry. This paper is organized as follows. In section 2, a simple coupled ocean–atmosphere model is constructed and analyzed. In section 3, we discuss results from a hybrid coupled GCM. A summary and discussion are given in section 4.

2. Analysis of coupled ocean–atmosphere instabilities

In this section, we intent to build a simple coupled model to assess the relative role of the aforementioned three types of coupled ocean–atmosphere instabilities. Our strategy is first to construct a model whose basic state is perfectly symmetric about the equator; then by introducing a perturbation that is antisymmetric about the equator, we examine how the perturbation grows under the symmetric basic state. To simplify the problem, we consider a two-dimensional model by assuming the zonal variations of model variables vanish.

a. The atmospheric model

The atmospheric model used here is Wang and Li's (1993) 2½-layer model that incorporates Gill's (1980) first-baroclinic mode free-atmosphere model with Lindzen–Nigam's (1987) boundary-layer model. It allows active interactions between free-atmosphere circulations driven by convective heating and boundary-layer flows driven by SST gradients. The basic state of the model atmosphere is a motionless, thermodynamic-equilibrium state that overlies a uniform SST distribution.

The governing equations of the 2½-layer model can be written as

TABLE 1. Parameters used in the simple coupled model.

Symbol	Parameter	Value
ϵ	Rayleigh friction/Newtonian damping coefficient in free atmosphere	10^{-5} s^{-1}
C_0	First-baroclinic gravity wave speed	50 m s^{-1}
I	Heating coefficient due to free-troposphere moisture convergence	0.63 (when SST = 27°C)
B	Heating coefficient due to boundary-layer moisture convergence	1.30 (when SST = 27°C)
d	Nondimensional depth of the boundary layer	0.25
G	Coefficient of longwave radiational forcing	6.9×10^{-4} m^2 s^{-3} K^{-1}
F	Coefficient of evaporation forcing	9.5×10^{-2} m s^{-2}
E	Ekman number of the boundary layer	2.7×10^{-5} s^{-1}
A	Coefficient of SST-gradient forcing	16 m^2 s^{-2} K^{-1}
H	Mean thermocline depth	30 m
H_1	Depth of the ocean mixed layer	100 m
g'	Reduced gravity in the upper ocean	0.05 m s^{-2}
r	Rayleigh friction coefficient of the mean upper ocean	1 yr^{-1}
r_s	Damping coefficient for Ekman shearing currents	1 day^{-1}

$$\frac{\partial U_L}{\partial t} - \beta y V_L = -\epsilon U_L, \tag{2.1}$$

$$\frac{\partial V_L}{\partial t} + \beta y U_L = -\frac{\partial \phi}{\partial y} - \epsilon V_L, \tag{2.2}$$

$$\frac{\partial \phi}{\partial t} + C_0^2(1 - \delta I)\frac{\partial V_L}{\partial y} = C_0^2 d(\delta B - 1)\frac{\partial V_B}{\partial y} - G(T_s - T_0) - \delta F|\mathbf{V}_s|(q_s - q_0) - \epsilon\phi, \tag{2.3}$$

$$EU_B - \beta y V_B = 0, \tag{2.4}$$

$$EV_B + \beta y U_B = -\frac{\partial \phi}{\partial y} + A\frac{\partial T_s}{\partial y}, \tag{2.5}$$

where (U_L, V_L) and (U_B, V_B) stand for the lower-troposphere and boundary-layer wind components, ϕ stands for the lower-troposphere geopotential height, $E = \rho_a g K_D/(p_s - p_e)$ is the Ekman number in the atmospheric boundary layer, $K_D = 2.3 \times 10^{-2}$ m s^{-1} is a surface friction coefficient, $p_e = 900$ mb denotes the pressure at the top of the boundary layer, $d = (p_s - p_e)/\Delta p$ represents the nondimensional depth of the boundary layer, $\Delta p = 400$ mb is the half pressure depth of the free troposphere, T_s represents sea surface temperature, and T_0 is the domain-averaged SST. Note that parameters I and B are heating coefficients related to free-troposphere and boundary-layer moisture convergences that are functions of total SST (the mean plus anomaly), whereas G and F are coefficients related to longwave radiational cooling and surface evaporation; $A = R(p_s - p_e)/2p_e$ represents SST-gradient forcing. [Detailed descriptions of the model parameters can be found in Wang and Li (1993).] Table 1 lists the values of key parameters in the simple atmospheric and oceanic models.

The precipitation rate in the model is determined by M, the sum of vertically integrated moisture convergences and local surface evaporation rate,

$$P_r = \delta M = \delta b\left[E_v - \frac{1}{g}\int_{pu}^{ps} \nabla\cdot(\bar{q}\mathbf{V})\, dp\right], \tag{2.6}$$

where

$$E_v = \rho_a C_D|\mathbf{V}_s|(q_s(T_s) - q_0) \tag{2.7}$$

is the rate of surface evaporation; $b = 0.75$ is a condensation efficiency coefficient measuring the fraction of total moisture convergence that condenses out as precipitation; $\bar{q}$ is the steady-state specific humidity that depends on the surface humidity q_0 and the pressure; $p_u = 100$ mb and $p_s = 1000$ mb denote the pressures at the top of troposphere and at the surface, respectively; $\rho_a = 1.2$ kg m^{-3} is the surface air density; $C_D = 1.4 \times 10^{-3}$ is a drag coefficient; $|\mathbf{V}_s|$ represents the model's lowest-layer wind speed; and $q_s(T_s)$ is the saturation specific humidity at sea surface temperature T_s. Air specific humidity at the surface is determined by SST based on a climatological monthly mean data analysis (Li and Wang 1994) via the empirical formula

$$q_0 = 10^{-3}(0.972T_s - 8.92). \tag{2.8}$$

In reality, convection occurs only when the atmosphere is convectively unstable. This requires a decrease with height of atmospheric equivalent potential temperature. From a statistical sense, this criterion is equivalent to an SST-dependent nonlinear heating scheme (Wang and Li 1993). Observational studies by Waliser and Graham (1993) have shown that on a monthly timescale atmospheric convection is highly correlated to SST. Therefore, in our current model an SST-dependent switch on coefficient δ is adopted. It is equal to one when the total moisture convergence M is greater than zero and SST is larger than 26°C and equal to zero otherwise.

The 2½-layer model of Wang and Li (1993) was intended to study the response of tropical low-level circulation to the underlying SST forcing. Given a uniform SST distribution, this model has a zero-wind solution. This solution is unrealistic since even in a homogeneous water-covered globe the angular momentum balance re-

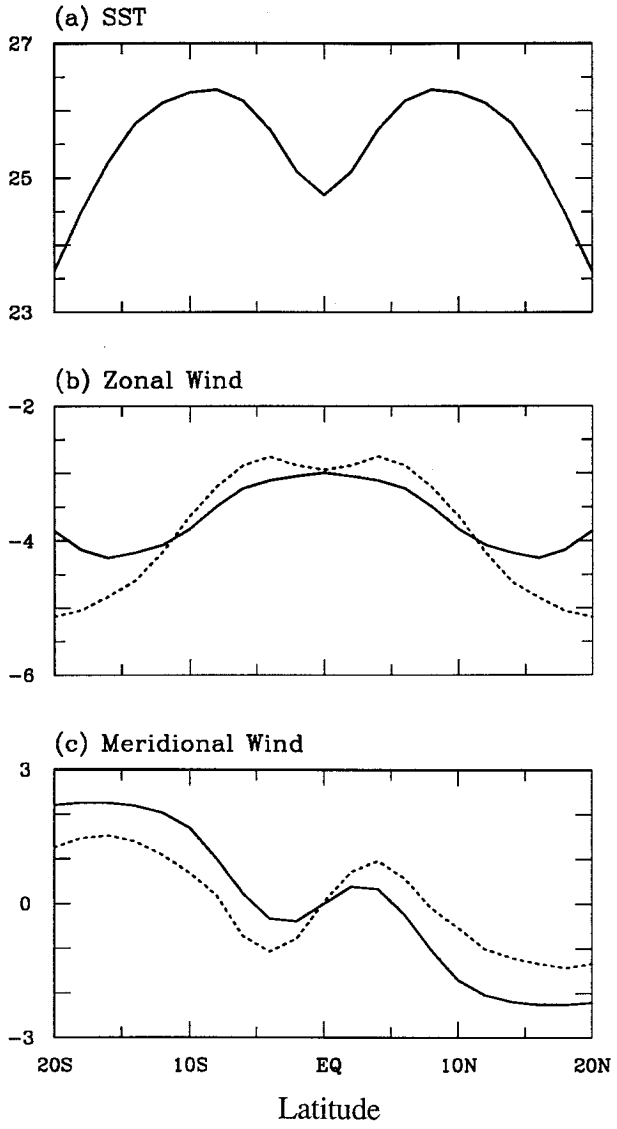

FIG. 2. The solid lines show the symmetric component of the observed annual mean (a) SST (°C), (b) zonal wind, and (c) meridional wind component (m s^{-1}) in the eastern Pacific (averaged between 140°W and 80°W). The dashed lines in (b) and (c) show the model-simulated wind components forced by SST in (a).

quires that westerly winds appear in the midlatitude and easterlies in the Tropics. The reason of this unrealistic aspect in the model is probably because of the absence of the nonlinear momentum transport by the Hadley circulation (Held and Hou 1980). So far, all simple Gill-type models fail to produce such a feature. Physically, the easterlies at the equator involve two distinctive modes: an air–sea coupled mode that involves feedbacks between the zonal wind and SST (which is related to the Walker circulation and the warm pool–cold tongue thermal contrast) and an ''external'' mode that does not involve air–sea coupling and is solely related to the angular momentum transport because of the rotation of the earth. As shown in our GCM experiments in the next section (see Fig. 9, for example), the external mode has approximately an amplitude of 3–4 m s^{-1} at the equator. To mimic the external mode effect in the model, a constant wind of -3 m s^{-1} is added to the model zonal surface wind component, following Xie and Philander (1994).

The dashed lines in Figs. 2b and 2c show the model response to the symmetric component of observed annual mean SST (averaged zonally between 140°W and 80°W, as shown in Fig. 2a) derived from the COADS (Comprehensive Ocean–Atmosphere Data Set). The solid lines in Figs. 2b and 2c illustrate their observed counterparts. The model is able to capture some important aspects of tropical surface wind variations.

b. The oceanic model

The oceanic model used in this study is a Cane–Zebiak-type model (Cane 1979; Zebiak and Cane 1987). This model was originally designed to study the El Niño–Southern Oscillation and further to study the seasonal cycle (Chang 1994; Li and Philander 1996). It describes the linear dynamics of a reduced-gravity upper ocean with a constant mixed layer. The vertical entrainment velocity at the base of the mixed layer is determined by the divergence of surface currents. The governing equations for the upper-ocean momentum, mass, vertical shearing current, and sea surface temperature anomalies (relative to a prescribed symmetric basic state) can been written as

$$\frac{\partial u_m}{\partial t} - \beta y v_m = \frac{\tau^x}{\rho H} - r u_m, \tag{2.9}$$

$$\frac{\partial v_m}{\partial t} + \beta y u_m = -g' \frac{\partial h}{\partial y} + \frac{\tau^y}{\rho H} - r v_m, \tag{2.10}$$

$$\frac{\partial h}{\partial t} + H \frac{\partial v_m}{\partial y} = -rh, \tag{2.11}$$

$$r_s u_s - \beta y v_s = \frac{\tau^x}{\rho H_1}, \tag{2.12}$$

$$r_s v_s + \beta y u_s = \frac{\tau^y}{\rho H_1}, \tag{2.13}$$

$$\frac{\partial T}{\partial t} = -v\bar{T}_y - \bar{v}T_y - [M(\bar{w} + w) - M(\bar{w})]\bar{T}_z - M(\bar{w})T_z + \frac{Q}{\rho C_w H_1}, \tag{2.14}$$

where (u_m, v_m) and (u_s, v_s) denote the mean upper ocean current and the vertical shearing current between the mixed layer and the layer below; $u = u_m + (H_2/H)u_s$ and $v = v_m + (H_2/H)v_s$ represent the surface current; H_1 and H are the mean mixed-layer and thermocline depths,

and $H_2 = H - H_1$; $w = H_1(\partial v/\partial y)$ is the vertical entrainment velocity at the base of the mixed layer; T_y and T_z are the meridional and vertical temperature gradients; $M(x)$ is a function that is equal to x when $x > 0$ and 0 when $x < 0$, representing a nonlinear nature of upwelling/downwelling in changing SST; Q denotes net heat flux anomaly at the surface, which is primarily determined by the shortwave radiation and latent heat flux anomalies; $\rho = 10^3$ kg m^{-3} represents the mean water density in the upper ocean; and $C_w = 4.2 \times 10^3$ m^2 s^{-2} K^{-1} is the specific heat of water. All quantities in Eqs. (2.9)–(2.14) with a bar denote the basic-state fields, and the others denote departures from this basic state.

c. The basic state, coupling, and numerical procedures

The basic state of the coupled model is specified as a symmetric (relative to the equator) component of observed climatological annual-mean SST, surface wind, and ocean temperature at 50 m, averaged zonally from 140°W to 80°W. The basic-state oceanic currents are then calculated from the oceanic model with the symmetric basic-state wind forcing.

The model atmosphere and ocean are coupled once per day. For simplicity a linearized wind stress formula is adopted, which has the form

$$\boldsymbol{\tau} = \rho_a C_D V_0 \, \mathbf{V}'_s, \tag{2.15}$$

where $V_0 = 5$ m s^{-1} represents a constant surface wind speed and $\mathbf{V}'_s$ denotes anomalous surface wind. The evaporation anomaly at the ocean surface can be written as

$$Q_{LH} = \rho_a C_D L_c[|\mathbf{V}'_s + \bar{\mathbf{V}}_s|(q_s - q_a) - |\bar{\mathbf{V}}_s|(\bar{q}_s - \bar{q}_a)], \tag{2.16}$$

where $\bar{\mathbf{V}}_s$ stands for the basic-state wind field; q_s and q_a are calculated from total sea surface temperature; $\bar{q}_s$ and $\bar{q}_a$ are computed from the basic-state SST; and $L_c = 2.5 \times 10^6$ J kg^{-1} represents latent heat of vaporization per unit mass.

Following Li and Philander (1996), an empirical formula is used to determine low-level marine stratus clouds. The shortwave radiation anomaly at the ocean surface can be expressed as

$$Q_{\mathrm{SW}} = [Q_0(1 - 0.62C) - Q_0(1 - 0.62\bar{C})] \times (1 - \lambda), \tag{2.17}$$

where Q_0 represents the annual-mean solar radiation at the top of the atmosphere, which is only a function of latitude; $C = -\alpha_1 T_s + \alpha_2$ and $\bar{C} = -\alpha_1 \bar{T}_s + \alpha_2$ denote the total and basic-state cloudiness, where $\alpha_1 = 0.7/13$, $\alpha_2 = 0.7/13 \times 29$; and $\lambda = 0.06$ denotes the surface albedo in the tropical ocean.

Two steps are needed to calculate the wind response to anomalous SST forcing. First, we obtain the response of the winds to the total SST (a sum of the prescribed basic-state SST and the SST anomaly) forcing. Then we subtract this solution from the basic-state solution obtained by forcing the model with the basic-state SST.

The model has a resolution of 1°, covering the region of 30°S–30°N. The lateral boundary condition is that the gradients of dependent variables vanish along the y direction.

The initial condition is an antisymmetric SST perturbation that has the form

$$T = \hat{T}\frac{y}{L}\exp\left(-\frac{y^2}{2L^2}\right), \tag{2.18}$$

where $L = 10°$ in latitude and $\hat{T} = 0.5 \exp(0.5)$. This perturbation has a maximum amplitude at $y = L$ and a minimum at $y = -L$. All other variables are set to be zero initially.

d. Instability analysis

Since the linear instability analysis is not proper (because of the nonlinearity of the model), we took a numerical approach by introducing a small perturbation initially and integrating the model forward. Growth rates are then calculated based on the time evolution of the SST anomaly. Because of the lack of advective nonlinearity, the system is ''quasi-linear''—exponentially growing solutions may exist for such a system (Charney and Eliassen 1964; Wang and Li 1994). To determine a time-mean growth rate, time integrations are carried out for 180 days. The growth rate is estimated from the maximum (minimum) amplitude of the SST anomaly and the time during which the maximum (minimum) is reached. Note that such a method may underestimate the growth rate, particularly when the initial perturbation is very different from the most unstable mode. To test the sensitivity of the growth rates to initial perturbations, we conduct a number of experiments, in the presence of the meridional wind–SST feedback, in which three different values of L ($L = 10°$, 8°, and 6°, respectively) are assigned. It turns out that the results are relatively insensitive to L.

The dashed line in Fig. 3 illustrates the time series of amplitude of the SST anomaly in the presence of the meridional wind–SST feedback (the evaporation–wind feedback and the cloud feedback are intentionally suppressed in this case). It clearly displays an exponential growth, with an *e*-folding timescale of 128 days. Figure 4a illustrates the meridional structure of the unstable SST mode (at day 180). It is an equatorially trapped, antisymmetric mode, with a characteristic length scale of 2°–3° latitude. In general, the structure of this mode resembles one obtained from a linear eigenvalue analysis by Chang and Philander (1994).

Figure 5a shows that the meridional wind–SST feedback strongly depends on the basic-state vertical temperature gradient in the upper ocean. Note that the upper portion of Fig. 5a corresponds to the condition in the eastern Pacific and Atlantic and the lower portion cor-

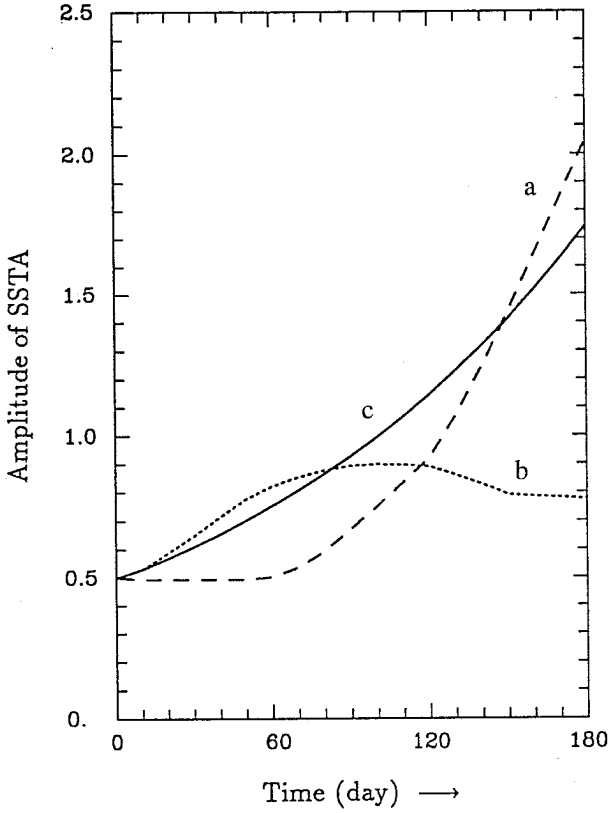

FIG. 3. The time evolution of amplitude of the SST anomaly (°C) in the presence of (a) the meridional wind–SST feedback (dashed line), (b) the evaporation–wind feedback (dotted line), and (c) the low-level stratus cloud–SST feedback (solid line) mechanisms.

responds to the condition in the western Pacific and the Indian Ocean. Therefore this positive-feedback mechanism is only effective in the eastern Pacific and Atlantic, not in the western Pacific and Indian Ocean. It is also sensitive to the depth of the atmospheric boundary layer and to the friction coefficients in both atmospheric and oceanic Ekman layers (Figs. 5a and 5b). In general, the growth rates are proportional to $\overline{T}_z$ and p_e, but oppositely proportional to r_s and E. The reason for the opposite proportion of the growth rate to r_s and E is straightforward—a larger dissipation leads to a smaller instability. A larger stratification, $\overline{T}_z$, causes a stronger vertical temperature advection and thus a colder SST for a given upwelling speed, which further intensifies the cross-equatorial wind and upwelling. In a dry atmosphere with the increase of boundary layer depth, more kinetic energy is dissipated. This is not a case in a moist atmosphere in which the frictional convergence heating increases more rapidly than the boundary layer dissipation [see detailed discussion in Wang and Li (1994)]. In a reasonable parameter regime the growth rates associated with the meridional wind–SST feedback have a typical *e*-folding timescale of 3–12 months.

The dotted line in Fig. 3 shows the time evolution of amplitude of the SST anomaly in the presence of the evaporation–wind feedback mechanism. (For this case the oceanic dynamics and the clouds are excluded.) It shows two distinctive time stages. The first stage is characterized by an exponential growth, accompanied by the equatorward movement of maximum SST and convection (Fig. 6); the second one is characterized by the maturity and decay of the perturbation. The growth rate during the first stage is estimated as approximately (120 day)$^{-1}$. From the latitude–time plot (Fig. 6) one can clearly see that the maximum SST moves southward from 10°N, gradually reaching a critical latitude (about 6°N) and staying along this latitude. Figure 4b illustrates the structure of the SST mode (at day 60) in the case.

One important question related to the evaporation–wind feedback is why it leads to an instability. We first consider a linear version of (2.1)–(2.16). Linearized by a uniform basic state for both the SST and the zonal wind components, the governing equation for a steady-state atmosphere in a constant f plane can be written as

$$\epsilon U_L - fV_L = 0, \tag{2.19}$$

$$\epsilon V_L + fU_L = -\frac{\partial \phi}{\partial y}, \tag{2.20}$$

$$\epsilon\phi + C_0^2(1 - \bar{I})\frac{\partial V_L}{\partial y} = C_0^2 d(\bar{B} - 1)\frac{\partial V_B}{\partial y} - GT - KU_B, \tag{2.21}$$

$$EU_B - fV_B = 0, \tag{2.22}$$

$$EV_B + fU_B = -\frac{\partial \phi}{\partial y} + A\frac{\partial T}{\partial y}, \tag{2.23}$$

$$\frac{\partial T}{\partial t} = -\frac{\rho_a C_D L_c \Delta q \bar{U}}{\rho C_w H_1 |\bar{U}|}U_B, \tag{2.24}$$

where $\bar{I} = I(\bar{T})$, $\bar{B} = B(\bar{T})$, $\Delta q = \bar{q}_s - \bar{q}_0$, and $K = (F - \Delta q \bar{U})/|\bar{U}|$ depend on the constant basic-state zonal wind, $\bar{U}$, and SST, $\bar{T}$. It is readily shown that the system (2.19)–(2.24) is absolutely stable. The phase speed of the system is a constant, independent of y, and the propagation direction depends on the sign of f and $\bar{U}$: a positive f and easterly wind ($\bar{U} < 0$) corresponds to southward propagation. In a constant β plane, the phase speed becomes more complicated and is a function of y. However, the stability feature remains unchanged (by solving an eigenvalue problem numerically).

It turns out that the instability in the model results from nonlinear atmospheric heating. Figure 7 illustrates the time tendency of SST at the initial time ($t = 0$) in the two cases—a linear case in which the moist static energy parameters I and B in (2.3) are only the function of the basic-state SST and the atmospheric heating is linear (i.e., $\delta \equiv 1$), and a nonlinear case in which I and B are the function of total SST and the heating coefficient δ depends on the total moisture convergence and SST. A much stronger tendency occurs, in the region of

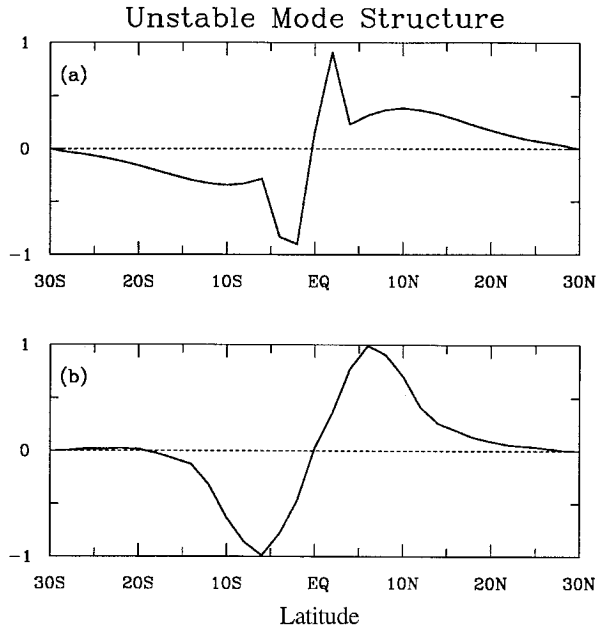

FIG. 4. The meridional structure of unstable SST modes in the presence of (a) the meridional wind–SST feedback (at day 180) and (b) the evaporation–wind feedback (at day 60). The SSTs have been normalized in terms of their maximum values so that the amplitudes are a unit.

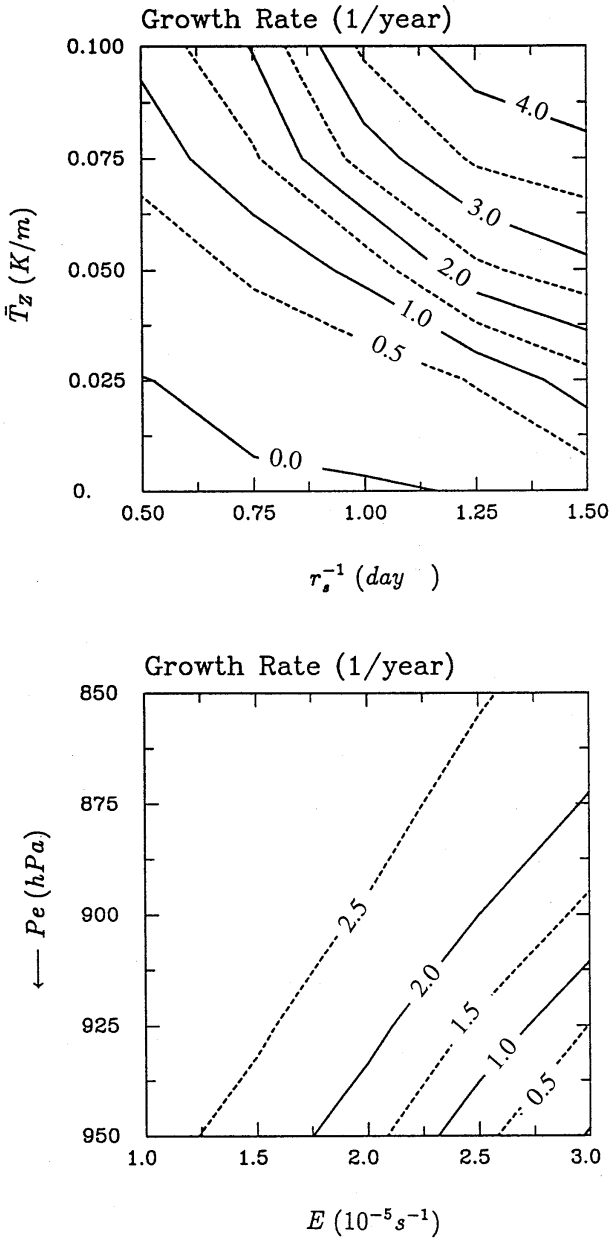

FIG. 5. Growth rates (yr^{-1}) as a function of (a) the basic-state vertical temperature gradient and friction coefficient in the ocean mixed layer and (b) the pressure at the top of the atmospheric boundary layer and the Ekman number in the presence of the meridional wind–SST feedback.

5°–10°N, in the case when the nonlinear heating is enabled.

The nonlinear heating destabilizes the system by the following two aspects: 1) An SST-dependent positive-only coefficient restricts the heating only in certain regions, which sharpens the pressure gradient, and 2) the terms that attained the moist static energy parameters I and B in (2.3) are essentially nonlinear—a positive SST anomaly not only induces the low-level moisture convergence that decreases the surface pressure but also reduces the static stability of the atmosphere. Both effects cause the stronger response of the winds for given SST forcing, which in turn changes the evaporation and thus SST. Because the nonlinear heating depends on the total (mean plus anomalous) moisture convergence and SST, the basic-state SST and winds may also contribute to the unstable growth of perturbations in the region of 5°–10°N where the basic-state moisture convergence and SST are maximum (Fig. 2).

The presence of equatorial upwelling and the cold tongue is essential to suppress the coupled instability and maintain an asymmetric structure. Without the cold tongue, the maximum SST and convection would eventually move to the equator (Xie and Philander 1994). In that case there is no equatorial asymmetry. Our numerical experiments show that this is the case in the western Pacific (figure not shown).

The third type of coupled ocean–atmosphere instability involves the low-level stratus cloud–SST feedback. In the absence of the dynamic coupling and the evaporation–wind feedback, one can readily derive the growth rate from (2.14) and (2.17), which is

$$\text{growth rate} = \frac{Q_0 0.62 \alpha_1 (1 - \lambda)}{\rho C_w H_1}. \qquad (2.25)$$

Equation (2.25) states that the growth rate depends on the cloud–SST feedback coefficient α_1, on the mixed layer depth H_1, and on the solar radiation at the top of the atmosphere Q_0. For given annual-mean insolation at

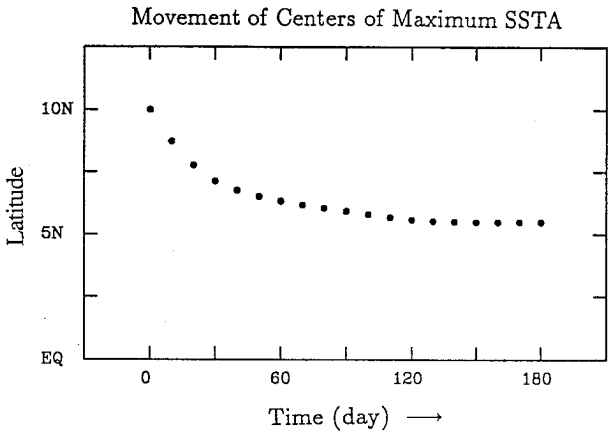

FIG. 6. The meridional movement of maximum SST anomalies in the presence of the evaporation–wind feedback mechanism. Initially, the SST perturbation is at 10°N.

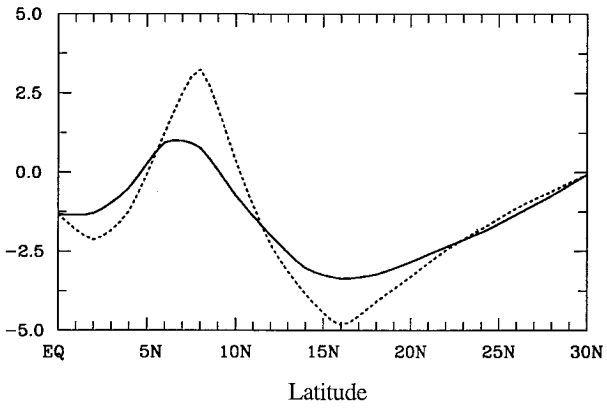

FIG. 7. The time tendency for SST (units: 10^{-8} K s^{-1}) at $t = 0$ in the cases of linear (solid line) and nonlinear (dotted line) atmospheric heating, in the presence of the evaporation–wind feedback.

10°N and a mixed layer depth of 30 m, the growth rate calculated from (2.25) is 2.4 yr^{-1}, close to the value of 2.5 yr^{-1} computed from the time integration. This adds confidence in taking a numerical approach to solve the model equations.

Figure 8 illustrates the growth rates, as a function of oceanic mixed layer depth, in the presence of the three types of coupled ocean–atmosphere instabilities: the meridional wind–SST feedback (dashed line), the evaporation–wind feedback (solid line), and the low-level stratus cloud–SST feedback (dotted line). For a reasonable parameter regime, the growth rates associated with the three coupled ocean–atmosphere instabilities are in the same order of magnitude, suggesting that they are all important in contributing to the climatic asymmetries relative to the equator. Figure 8 shows that the smaller the oceanic mixed layer depth, the larger the coupled instabilities. The reason for that is quite simple for the evaporation–wind feedback and the stratus cloud–SST feedback since the heat flux term in the SST equation is always divided by H_1. The most important term in changing SST in the presence of the meridional wind–SST feedback is $-wT_z$. Since $w \propto (H - H_1)/H$, a smaller mixed layer depth leads to a stronger vertical temperature advection and therefore a larger instability. For a given oceanic mixed-layer depth ranging from 20 to 50 m, the growth rates have values of 1.5–4.0 yr^{-1}, which corresponds to an *e*-folding timescale of 100–300 days.

To sum up, interactions between the ocean and atmosphere mentioned earlier can amplify the asymmetry introduced initially. These interactions only work in the eastern Pacific and Atlantic because they strongly depend on the existence of a shallow oceanic mixed layer, which in turn is a result of equatorial easterlies. Therefore, the existence of the equatorial easterlies is a necessary condition for the amplification of the climatic asymmetry.

3. Experiments in a hybrid coupled GCM

In the previous section, we investigated air–sea interactions in a simple model without considering land and coastal effects. In this section, we use a more realistic, hybrid coupled GCM in which a realistic continental and coastal distribution is presented. The atmospheric model used in this study is the Geophysical Fluid Dynamics Laboratory (GFDL) global GCM (R30 model) and is essentially the one described by Manabe and Hahn (1981). The oceanic model is a modified Cane–Zebiak model [modified in the sense that the model considers the heat fluxes at the surface and predicts total rather than anomalous SST; see Chang (1994) for details]. They are coupled once per day. The oceanic model has a horizontal resolution of 2° in longitude and 1° in latitude, covering the global Tropics from 30°S to 30°N; beyond the latitudes, SST is specified from the symmetric component of the observed annual-mean field. In all of the following cases the annual-mean solar radiation at the top of the atmosphere, which is approximately symmetric about the equator, is specified.

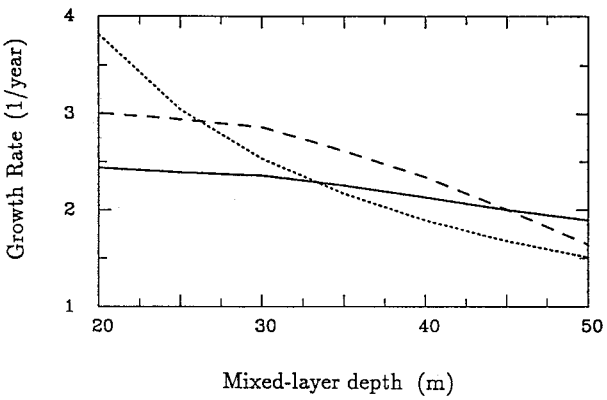

FIG. 8. Growth rates (yr^{-1}) as a function of the oceanic mixed-layer depth in the presence of the meridional wind–SST feedback (dashed line), the evaporation–wind feedback (solid line), and the stratus cloud–SST feedback (dotted line) mechanisms.

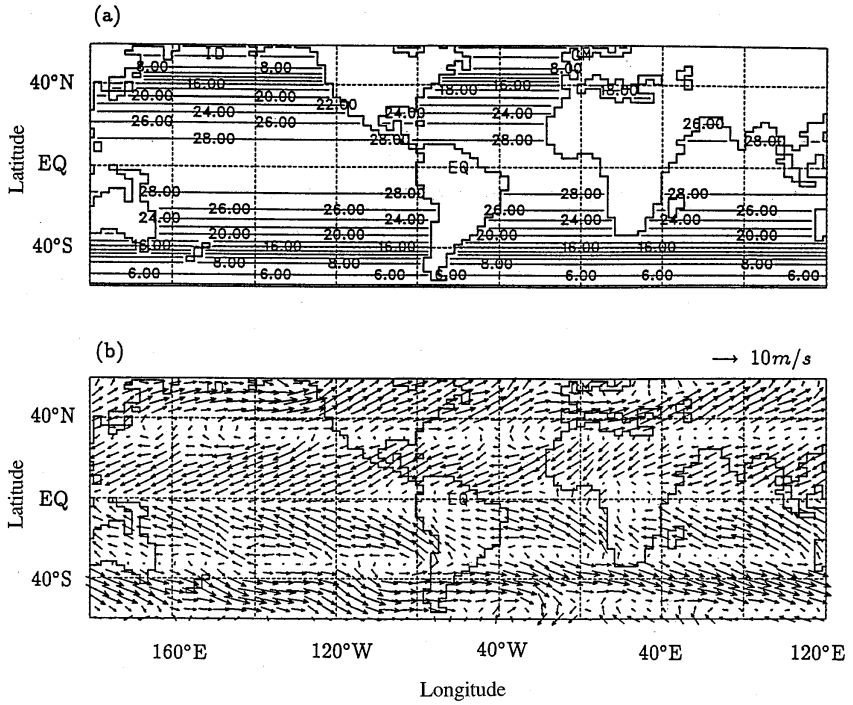

FIG. 9. (a) A prescribed zonal-mean symmetric SST (°C) field derived from the climatological monthly mean COADS dataset (averaged between 140°E and 180°). (b) The R30-model simulated surface wind field forced by the above prescribed symmetric SST and the annual-mean solar radiation.

The asymmetric climate in the nonlinear hybrid coupled GCM can be regarded as a nonlinearly equilibrated state of the low-latitude climate system. There must be twin (mirror image) asymmetric solutions if boundary conditions are symmetric. The questions we need to address here are the following: What is the role of the continental asymmetry in determining the asymmetric climate solution? Can the asymmetry of continents alone (without the involvement of air–sea interactions) cause the observed response of the asymmetric winds? To answer these questions we start from an uncoupled case in which a zonal-mean symmetric SST field (as shown in Fig. 9a) is specified as the atmospheric lower boundary condition. This symmetric SST condition can be viewed as a direct response of the ocean to the annual-mean solar forcing. Figure 9b illustrates the model wind field in this case. Note that in the tropical Atlantic an equatorial asymmetry, characterized by a northward cross-equatorial wind component, has been established. Such an asymmetry results directly from land–ocean thermal contrast, because of higher land surface temperature in the bulge of northwestern Africa. The winds over the eastern Pacific, however, remain symmetric about the equator, and there is no cross-equatorial wind component. The results suggest that the greater land mass in the Northern Hemisphere does not contribute to the ITCZ asymmetry in the eastern tropical Pacific.

Two important features in the surface wind field in the tropical Pacific are worth noting. First, there are strong easterlies at the equator even though the SST does not vary zonally. (Keep in mind that all simple models fail to simulate this feature.) Such winds, when allowed to influence the ocean, can drive the warm surface waters westward and upwell the cold water from below to the surface in the east, resulting in a strong east–west asymmetry in SST (the warm pool–cold tongue thermal contrast). (It has been shown in the previous section that the equatorial easterly is a fundamental factor to determine the ocean–atmosphere instabilities.) Second, because of the tilt of the America coast, the trade winds to the south (north) of the equator are essentially parallel (perpendicular) to the coast. As we know, the parallel-to-coast winds may induce strong upwelling along the coast and cool SST there. Therefore, when coupled to the ocean, the winds can cause anomalous cooling off the coast of Peru but anomalous warming off the coast of Panama, which initiates an equatorial asymmetry. Once the equatorial asymmetry is initiated, the ocean–atmosphere interactions mentioned earlier could further amplify the asymmetry to reach the observed strength.

To test the idea, we conduct sets of coupled experiments. In the first set of experiments, we focus on the dynamic coupling (in the sense that the atmosphere influences the ocean solely through wind stresses without the involving of thermodynamic or heat flux processes) by simply suppressing evaporation and cloud effects. The heat fluxes at the ocean surface are specified as a

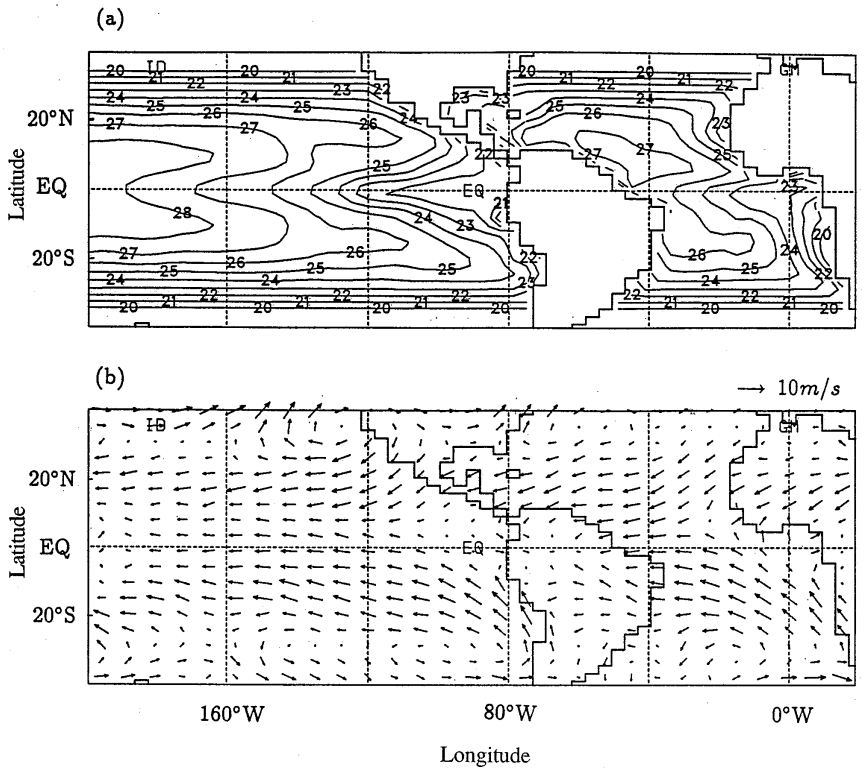

FIG. 10. The simulated (a) SST (°C) and (b) surface wind fields from a hybrid coupled GCM. Only the dynamic coupling is considered in this case. The thermodynamic coupling, such as the surface evaporation and cloud effects, is intentionally suppressed. The model starts from a symmetric SST condition as shown in Fig. 9a.

Newtonian damping term (restoring the surface temperature toward a prescribed symmetric SST field, as shown in Fig. 9a), which is

$$\text{heat flux} = -\frac{T - T_{\text{sym}}}{\tau_0}, \tag{3.1}$$

where τ_0 is a Newtonian damping timescale that is set to be 180 days. The model starts from a symmetric SST condition (as shown in Fig. 9a) and initially there is no motion in both the ocean and atmosphere. Because of the establishment of equatorial easterlies, an east–west asymmetry, characterized by a warm pool in the western Pacific and a cold tongue in the eastern Pacific (Fig. 10a), is established. Because of the tilt of the western coasts of the Americas, a north–south SST asymmetry develops. It can be easily seen from the model surface wind field (Fig. 10b) that there is a northward cross-equatorial wind component in the eastern Pacific.

The dynamic coupling in the model contains two important, distinctive processes: 1) a coastal wind-upwelling mechanism that perturbs SST in the vicinity of the coastal regions and is responsible for the initiation of an equatorial asymmetry and 2) the meridional wind–SST feedback that amplifies the asymmetry through positive feedbacks. The former is a coastal mode that may involve air–sea interactions in the vicinity of the coast and the latter is an equatorially trapped mode whose meridional extent is confined by a frictional characteristic length scale, $L = \sqrt{Er_s/\beta}$ (Chang and Philander 1994).

To demonstrate the importance of the coastal wind-upwelling mechanism in initiating the equatorial asymmetry, we conduct an ideal experiment in which the western coasts of the Americas are parallel to a longitude. Our results show that in the absence of the coastal wind-upwelling mechanism there is no equatorial asymmetry in the eastern tropical Pacific.

To quantitize the extent of the asymmetry, an equatorial asymmetry index is introduced as

$$A_e = \langle V \rangle (\langle T \rangle_{\text{N}} - \langle T \rangle_{\text{S}}), \tag{3.2}$$

where $\langle V \rangle$ denotes a mean (averaged between 5°S and 5°N) cross-equatorial wind component and $\langle T \rangle_{\text{N}}$ and $\langle T \rangle_{\text{S}}$ stand for, respectively, mean ocean surface temperatures between 10°N and 0° and between 0° and 10°S. The solid line in Fig. 11 shows the index in this case.

In the second set of experiments, we consider both the dynamic coupling and surface evaporation. The reason to consider the combined effect, rather than the evaporation only, is that the evaporation–wind feedback alone can not generate an asymmetry in the eastern Pacific, even though a realistic continental distribution

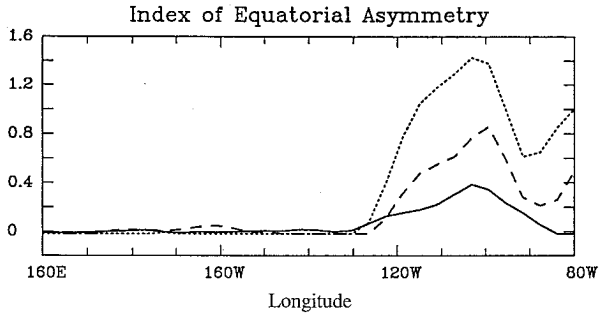

FIG. 11. The longitudinal distribution of the equatorial asymmetry index (°C m s^{-1}) in the three cases: the dynamic coupling (solid line), the dynamic coupling plus the evaporation–wind feedback (dashed line), and the combined dynamic coupling, evaporation–wind feedback, and low-level stratus cloud–SST feedback (dotted line).

is presented. This is because the evaporation depends on both the surface wind speed and the air–sea specific humidity difference (the latter is primarily the function of SST). Therefore the winds and SST will remain symmetric if initially they are so. The same is true for the stratus cloud–SST feedback because the clouds in the model depend on the atmospheric low-level static stability and on vertical motion that are somehow related to the SST and winds.

A simple way to demonstrate the role of evaporation–wind feedback in a coupled GCM is to decompose the total surface latent heat flux into a symmetric and an antisymmetric part and only let the antisymmetric component influence the SST. The symmetric part, together with other flux terms (i.e., the solar radiation, the longwave radiation, and the sensible heat fluxes), is assumed to have a Newtonian cooling formula that forces the model SST toward a symmetric field (as shown in Fig. 9a). The total heat flux at the ocean surface can then be written as

$$\text{heat flux} = -\text{LH}_{\text{antisym}} - \frac{T - T_{\text{sym}}}{\tau_0}, \qquad (3.3)$$

where $\text{LH}_{\text{antisym}}$ denotes the antisymmetric component of the latent heat flux at the surface. The model restarts from the previous case. Because of the presence of the evaporation–wind feedback, the equatorial asymmetry intensifies, which can be seen from the dashed line in Fig. 11.

The third set of experiments combines the three processes (the dynamic coupling, the evaporation–wind feedback, and the low-level stratus cloud–SST feedback) together. We specify the surface heat flux as follows:

$$\text{heat flux} = \text{SW}_{\text{antisym}} - \text{LH}_{\text{antisym}} - \frac{T - T_{\text{sym}}}{\tau_0}, \qquad (3.4)$$

where $\text{SW}_{\text{antisym}}$ denotes the antisymmetric component of the shortwave radiation at the surface. Following Philander et al. (1996), an empirical formula for the low-level stratus clouds (derived based on observations and GCM simulations) is adopted in which the clouds depend on both the low-level static stability and the vertical motion. The clouds in the model tend to form over the extremely cold SST tongue regions and appear more south than north of the equator. This leads to less shortwave radiation (into the ocean) in the Southern than Northern Hemisphere, magnifying the existing asymmetry. The dotted line in Fig. 11 indicates that this is the case in which the low-latitude climate in the coupled ocean–atmosphere system is most asymmetric. Figure 12 shows the simulated SST and wind fields in this case. A strong cold tongue, with a minimum of 21°C at the equator, occurs in the eastern tropical Pacific, resembling well the observed structure. Accompanying the SST are the strong northward cross-equatorial winds that converge onto the ITCZ north of the equator.

To sum up, in the presence of dynamic coupling, the evaporation–wind feedback, and the low-level stratus cloud–SST feedback the coupled model is capable of reproducing a realistic asymmetric time-mean state in the eastern Pacific and Atlantic. The asymmetry is set up by the continental asymmetry and amplified through the ocean–atmosphere interactions. The most important reason for the ITCZ to stay north of the equator is the bulge of northwestern Africa for the Atlantic and the tilt of the western coast of the Americas for the Pacific.

4. Summary and discussion

In this paper, we investigated the relative role of three types of coupled ocean–atmosphere instabilities—the meridional wind–SST feedback, the evaporation–wind feedback, and the low-level stratus cloud–SST feedback—in contributing to the climatic asymmetry relative to the equator. The scope of this study is twofold. First, we constructed a simple analytical model and evaluated the growth rates associated with the three coupled ocean–atmosphere instabilities in a unified dynamic framework. Second, we used a hybrid coupled GCM, in which a realistic land and coastal geometry is presented, to understand the processes that initiate an equatorial asymmetry and the mechanisms that amplify the asymmetry. The principal result is that the three types of air–sea interaction mechanisms are all important in amplifying the climatic asymmetry set up by the continental asymmetry.

So far three types of coupled ocean–atmosphere instabilities relative to the ITCZ have been proposed and studied separately. The relative importance of these feedback processes is not clear. The purpose of this study is to understand and compare these mechanisms in a unified dynamic framework. To achieve the goal, a simple coupled model was built in which the atmospheric component is Wang and Li's (1993) 2½-layer model and the oceanic component is a Cane–Zebiak type model. Our strategy has been to linearize the coupled model about a symmetric basic state and to examine

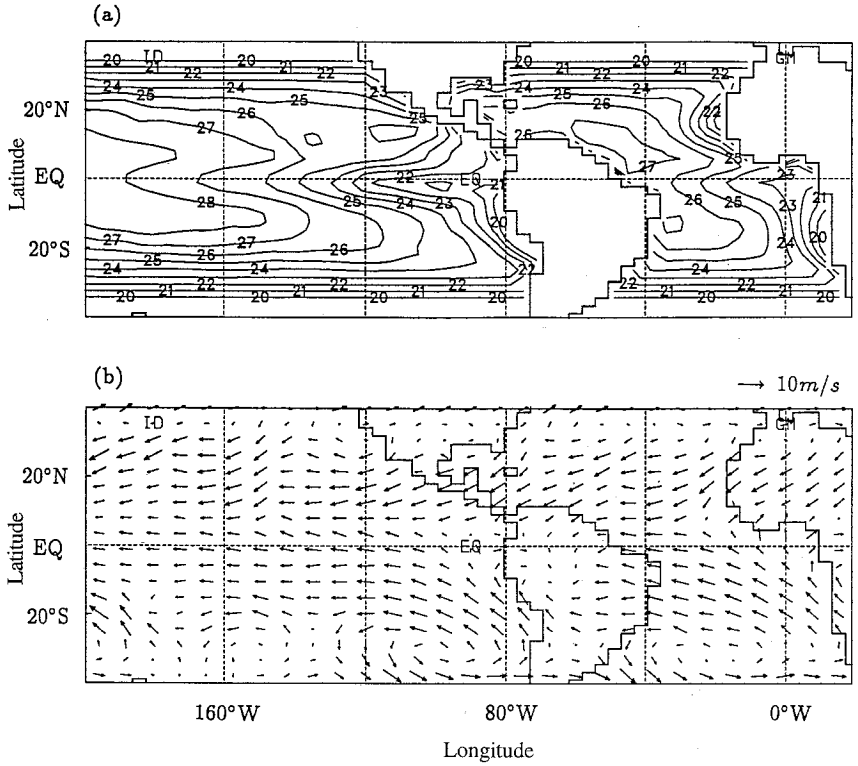

FIG. 12. The simulated (a) SST (°C) and (b) surface wind fields from the hybrid coupled GCM in the presence of the dynamic coupling, the evaporation–wind feedback, and the low-level stratus cloud–SST feedback.

under what conditions the symmetric basic state is unstable to a perturbation that is antisymmetric about the equator and how fast it can grow. Because of nonlinearity of the model, we took a numerical approach to calculate growth rates. Our results indicate that in a reasonable parameter regime the growth rates associated with the three coupled ocean–atmosphere instabilities are of the same order of magnitude, suggesting that they are all important in contributing to the climatic asymmetry relative to the equator.

The meridional wind–SST feedback depends strongly on the basic-state ocean thermal structure—the larger the mean upper-ocean vertical temperature gradient, the stronger the instability. Because of the dependence, this mechanism is only effective in the eastern Pacific and Atlantic where the mixed layer in the ocean is shallow, not in the western Pacific and Indian Oceans. In the presence of the evaporation–wind feedback, the equatorial upwelling ''saves'' the asymmetry by keeping the maximum SST away from the equator. The positive feedback between the stratus cloud and SST also works only in the eastern Pacific and Atlantic where SST is extremely cold. It turns out that all three positive-feedback processes are dependent on the existence of a shallow mixed layer that, in turn, is a result of equatorial easterlies. Therefore, the existence of the equatorial easterlies is a fundamental cause for the amplification of the ITCZ asymmetry.

A particularly important question regarding the climatic asymmetry is why the ITCZ is most favorable for the Northern Hemisphere. The positive feedbacks between the atmosphere and ocean can favor either hemisphere. The answer to the question must involve the asymmetry of continents. In the second part of the study we addressed this issue by conducting a number of coupled experiments using a hybrid coupled GCM in which a realistic continental and coastal distribution is described. The atmospheric model is the GFDL's R30 general circulation model, whereas the oceanic model is a Cane–Zebiak type model. We started from an uncoupled case in which an ideal, zonal-mean symmetric SST field (resembling that in the western Pacific) is specified, as the atmospheric lower boundary condition. The only force is the annual-mean insolation at the top of the atmosphere, which is approximately symmetric about the equator. Our results show that an asymmetry is readily generated in the Atlantic because of the land–ocean thermal contrast as the northwestern Africa land surface attains a much higher temperature than that of the ocean to its south. The winds over the eastern Pacific, however, remain symmetric about the equator. It is found that a coastal wind-upwelling mechanism is critical for per-

turbing SST in the vicinity of the coastal region and initiating an equatorial asymmetry. Because the trade winds along the tilted western coast of South America are essentially parallel to the coast, which induces strong upwelling off the coast of Peru, a north–south asymmetry is established. Once the asymmetry is introduced, the ocean–atmosphere interactions mentioned earlier further amplify the asymmetry. In the presence of these mechanisms, our model is able to simulate a realistic asymmetric time-mean state in the eastern Pacific and Atlantic.

Simulation of a realistic time-mean state is essential for a coupled GCM to predict seasonal-to-interannual variability. At the moment a few such models are being developed and have shown some degree of difficulty (K. Miyakoda 1995, personal communication). Statistics of 11 coupled GCMs around the world reveal a common success in simulating the east–west asymmetry (the warm pool–cold tongue contrast) and trouble in simulating the north–south asymmetry (Mechoso et al. 1995). Some of these models produced double ITCZs. A serious problem that has been commonly found is the failure to predict very thin marine low-level stratus clouds off the coasts of Peru and California; thus an important feedback mechanism is missing in these models. The parameterization of such clouds in our current model is simple and crude; it deserves further research. An asymmetric climate must have a twin (mirror image) solution if boundary conditions are symmetric. When boundary conditions are set asymmetric, there may be only one solution. However, it is not guaranteed, and there may be still twin solutions for even this case. (Twin solutions, of course, are not mirror images for this case.) Applying this argument to the coupled GCM simulations, one may wonder whether or not a climate with ITCZ in the Southern Hemisphere can exist even with the realistic asymmetric geography. In this paper we solely consider the response of a coupled ocean–atmosphere system to the annual-mean solar radiation forcing, neglecting the effect of the seasonal varying solar radiation. As shown in our stability analysis, all three instability processes produce a rather slow growth: the *e*-folding time ranges from 3 to 12 months. It is possible that the presence of the annually varying asymmetric forcing may alter these slow coupled instabilities. All these issues will be pursued in future studies.

Acknowledgments. The author would like to thank Dr. G. Philander for stimulating discussions and two anonymous reviewers for their insight and comments, which helped improve the manuscript. Comments given by Drs. S. Manabe, I. Held, G. Lau, B. Wang, P. Chang, S. Xie, G. Lambert, D. Neelin, S. Chang, T. Hogan, and C. Reynolds are greatly appreciated. Part of this work was done while the author was a visiting scientist at the Atmospheric and Oceanic Sciences Program of Princeton University, supported by NOAA Grant NA26G0102-01 and NASA Grant NASANAG 5-2224. Additional work was supported by the Office of Naval Research under program element 0601153N-R3103. The author acknowledges the use of computer facilities at the Geophysical Fluid Dynamics Laboratory and thanks Mr. S. Bishop for his editorial assistance.

REFERENCES

Cane, M. A., 1979: The response of an equatorial ocean to simple wind stress patterns. I: Model formulation and analytic results. *J. Mar. Res.,* **37,** 233–252.

Chang, P., 1994: A study of seasonal cycle of sea surface temperature in the tropical Pacific Ocean using reduced gravity models. *J. Geophys. Res.,* **99** (C4), 7725–7741.

——, and S. G. H. Philander, 1994: A coupled ocean–atmosphere instability of relevance to seasonal cycle. *J. Atmos. Sci.,* **51,** 3627–3648.

Charney, J. G., and A. Eliassen, 1964: On the growth of the hurricane depression. *J. Atmos. Sci.,* **21,** 68–75.

Emmanuel, K. A., 1987: An air–sea interaction model of intraseasonal oscillation in the tropics. *J. Atmos. Sci.,* **44,** 2324–2340.

Gill, A. E., 1980: Some simple solutions for heat-induced tropical circulation. *Quart. J. Roy. Meteor. Soc.,* **106,** 447–462.

Held, I. M., and A.Y. Hou, 1980: Nonlinear axially symmetric circulations in a nearly inviscid atmosphere. *J. Atmos. Sci.,* **37,** 515–533.

Li, T., and B. Wang, 1994: A thermodynamic equilibrium climate model for monthly mean surface winds and precipitation over the tropical Pacific. *J. Atmos. Sci.,* **51,** 1372–1385.

——, and S. G. H. Philander, 1996: On the annual cycle of the eastern equatorial Pacific. *J. Climate,* **9,** 2986–2998.

Lindzen, R. S., and S. Nigam, 1987: On the role of sea surface temperature gradients in forcing low-level winds and convergence in the tropics. *J. Atmos. Sci.,* **44,** 2418–2440.

Manabe, S., and D. G. Hahn, 1981: Simulation of atmospheric variability. *Mon. Wea. Rev.,* **109,** 2260–2286.

Mechoso, C. R., and Coauthors, 1995: The seasonal cycle over the tropical Pacific in coupled ocean–atmosphere general circulation models. *Mon. Wea. Rev.,* **123,** 2825–2838.

Mitchell, T. P., and J. M. Wallace, 1992: On the annual cycle in equatorial convection and sea surface temperature. *J. Climate,* **5,** 1140–1152.

Neelin, J. D., 1991: The slow sea surface temperature mode and the fast-wave limit: Analytic theory for tropical interannual oscillation and experiments in a hybrid coupled model. *J. Atmos. Sci.,* **48,** 584–606.

——, I. M. Held, and H. Cook, 1987: Evaporation-wind feedback and low-frequency variability in the tropical atmosphere. *J. Atmos. Sci.,* **44,** 2341–2348.

Philander, S. G. H., D. Gu, D. Halpern, G. Lambert, G. Lau, T. Li, and R. C. Pacanowski, 1996: Why the ITCZ is mostly north of the equator. *J. Climate,* **9,** 2958–2972.

Schopf, P. S., and M. J. Suarez, 1988: Vacillations in a coupled ocean–atmosphere model. *J. Atmos. Sci.,* **45,** 549–566.

Waliser, D. E., and N. E. Graham, 1993: Convective cloud systems and warm-pool SSTs: Coupled interactions and self-regulation. *J. Geophys. Res.,* **98,** 12 881–12 893.

Wang, B., and T. Li, 1993: A simple tropical atmosphere model of relevance to short-term climate variations. *J. Atmos. Sci.,* **50,** 260–284.

——, and ——, 1994: Convective interaction with boundary-layer dynamics in the development of a tropical intraseasonal system. *J. Atmos. Sci.,* **51,** 1386–1400.

Xie S.-P., 1994: The maintenance of an equatorially asymmetric state in a hybrid coupled GCM. *J. Atmos. Sci.,* **51,** 2602–2612.

——, and S. G. H. Philander, 1994: A coupled ocean–atmosphere model of relevance to the ITCZ in the eastern Pacific. *Tellus,* **46A,** 340–350.

Zebiak, S. E., and M. A. Cane, 1987: A model ENSO. *Mon. Wea. Rev.,* **115,** 2262–2278.